

## Modelling of Coal Pyrolysis Using a Twin Screw Reactor

Michael K. Roedig, Wolfgang Klose

University of Kassel, Institute of Thermal Engineering, Germany

[mk.roedig@uni-kassel.de](mailto:mk.roedig@uni-kassel.de)

Based on the balance equations of mass, partial mass, momentum and thermal energy, the pyrolysis process of non-coking coals using a counter-rotating twin screw reactor (TSR) is modelled by means of commercial CFD code Phoenix<sup>TM</sup>. In favour of good convergence of the mathematical solution, a structured, cylindrical-polar grid is chosen. Variable filling and intermeshing degrees are taken into account by blocking numerical cells in gas domain and intermeshing domain instead of performing two-phase calculations in a body-fitted co-ordinate system. Viscous behaviour of the granular coals is expressed by means of a generalised Newtonian fluid and chemical decomposition is implemented with aid of distributed activation energies.

### Introduction

Iron ore reduction is largely carried out in the blast furnace process which relies on input of coke. Due to shortness of coking coals, expensive upgrading in the coke oven battery and political conditions to lower emissions of carbon dioxide (CO<sub>2</sub>), several alternative processes based on smelting reduction and direct reduction are under way. In scope of the European Ultra-Low CO<sub>2</sub> Steelmaking project (ULCOS), a continuous ore reducing process is currently being developed (M. B. Denys, B. Smith [1]). The process incorporates partial pyrolysis of non-coking coals in a counter-rotating twin screw reactor (TSR) prior being fed into an ore smelting cyclone as a fuel and reducing agent. Direct reduction in a mixed iron-coal smelting bath, combined with carbon capture and storage technology (CCS) is expected to lower specific CO<sub>2</sub> emissions up to 50 % in comparison to common blast furnace processes. The purpose of the TSR is to preheat and upgrade low cost feed coals by partial pyrolysis, which is to increase specific carbon fraction by lowering specific hydrogen and oxygen fractions while heating the reactor by combustion of pyrolysis gases. In order to determine preferable TSR designs and working conditions, occurring transport phenomena are investigated by means of a mathematical model using CFD code Phoenix<sup>TM</sup>. A basic counter-rotating TSR design is shown in **Figure 1**.

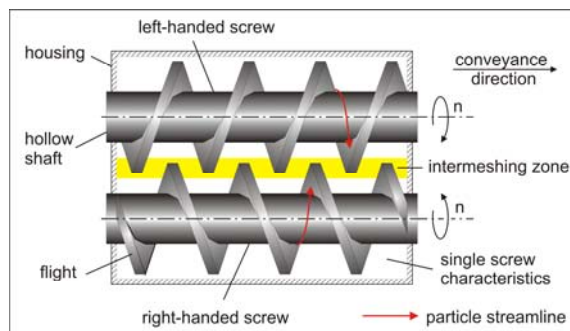


**Figure 1.** Basic TSR design

The TSR consists of a right-handed and left-handed screw, paired in a single housing. Conveyance of the coal charge is caused by contrary rotation of screws, thus, stresses being exerted at the coal charge boundary interfaces. Red arrows in **Figure 1** indicate particle streamlines in case of non-slip boundary conditions. To accelerate indirect heating of the coal charge, hot flue gases will be carried counter flow along the reactor housing as well as through the hollow shafts of the screws.

Due to complexity of the twin screw design, modelling is very challenging and some simplification reasonable. On one hand, it accounts for economy of numerical calculations; on the other hand, some substantial uncertainties arise from rheological modelling of the granular coal charge, putting the benefit of a highly detailed grid into question. In this context, formulation of the viscous stress tensor and choice of the boundary conditions are supposed to dominate macroscopic modelling results like total mass flow and heat flux, rather than type of grid.

Rheological behaviour of granular coals is barely documented and modelling even becomes more complicated, if drying and chemical decomposition is involved. Pure screw conveyors are usually operated at filling degrees up to roughly 45 % in order to achieve defined mass flow almost independent on rheological properties of the transported granular material. Since in this case, conveyance occurs in separated c-shaped chambers and no material is transported over top of the shaft, mass flow is following a linear dependency on rotational speed, cross-sectional area, pitch and bulk density. While this configuration allows for high mass flow, particle mixing is expected to be rather poor. Following, heat transport into the charge is assumed to be nearby pure effective thermal conductivity of the granular coals, which is around 0.1 - 0.5 W/(mK) and long residence times are needed to obtain homogeneous heating (J. Marth [2]).

At higher filling degrees, this basic derivation of mass flow as demonstrated above is no longer valid in

principle, but it can be considered as a limiting case. Being aware of the difficulties resulting from rheology modelling, the claim of the mathematical model is to indicate potentials and limits of the TSR technology as an auto-thermal coal upgrading process.

### Single Screw Modelling

A first goal in screw modelling was to understand transport phenomena occurring in the fully filled single screw, before moving on to the more complex design of the partially filled, intermeshed twin screw. For this purpose, the helical single screw channel is unwound, resulting in a planar u-shaped channel of rectangular cross-sectional area at rest and a sliding plate (cp. tubular housing) on top, as proposed by F. Hensen et al. [3]. This means, the velocities at the channel walls are always set to zero, while the plate moves with maximum speed, which is derived from rotational speed and diameter of the screw. Afterwards, no-slip and slip velocity boundary conditions are attached to the channel and the plate for calculation of limiting cases. As a general rule, conveyance is result of relative movement between the charge and the screw.

Therefore, applying full slip conditions to the screw and no-slip condition to the plate yields maximum throughput and the charge remains non-sheared. With this setting, the co-axial plug flow of charge in the real screw is transformed into a longitudinal plug flow in the planar channel model. This case could be exemplified best by holding a nut at rest while turning the thread.

Formulating no-slip conditions at all boundaries results in shearing of the charge with a typical velocity distribution: According to boundary conditions, low velocities exist nearby the screw channel while the highest velocities are obtained nearby the moving plate. For the quadratric cross sectional channel, throughput of a Newtonian fluid is about 36 % of maximum throughput.

Applying full slip at the plate results in zero relative movement between screw and the charge and therefore, pure rotation of the charge. In this case, throughput is zero.

### TSR Grid Design

Afore described concept of single screw modelling is also applied for twin screw modelling. Instead of using a body-fitted grid, local grid modifications are attached to the single screw to account for partial filling and the effect of the second screw. This choice was made to benefit from rapid grid generation as well as calculation accuracy as a result of grid orthogonality.

One of the main drawbacks of the planar channel concept is the inappropriate reproduction of ratio between the cylindrical shell areas (shaft and housing), which generate errors in total heat flux and momentum flux. Therefore, a cylindrical co-ordinate system was chosen and the helical channel of the real screw is represented by a series of numerically

linked annuli which make up the co-axial extension (**Figure 3**). The thickness of each annulus corresponds to the pitch of the screw. This means, velocities, temperatures and mass fractions of the coal charge reaching the outlet of a ring are formulated as inlet boundary conditions at the adjacent downstream ring.

To model variable volumetric filling degrees, numerical flow domain is partially restricted by blocking cells above filling height level, meaning these cells are impenetrable to flow. Because conveyance of the granular phase is of primary interest and in favour of numerical calculation, the model is single-phase. Due to marginal shrinking of the coal charge, filling level is presumed to be constant. As no substantial interaction between gas-phase and coal-phase takes place, shear stress is set to zero at the phase boundary plane denoted B-B (**Figure 2**).

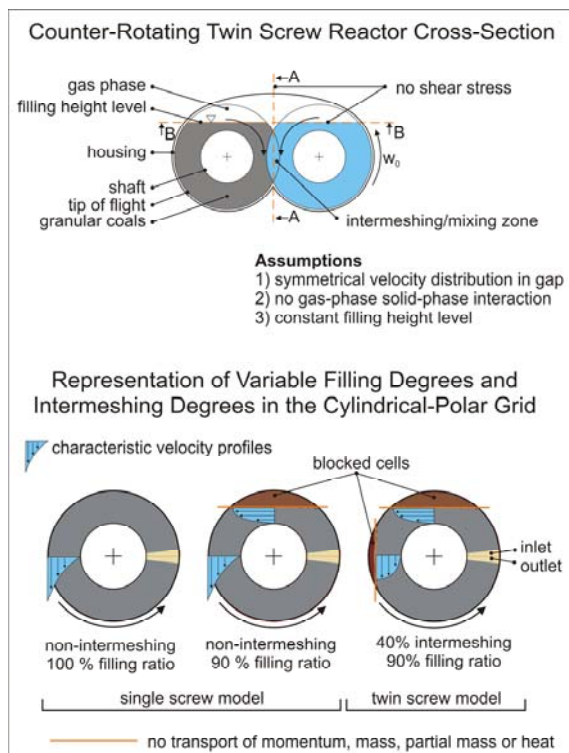


**Figure 2.** Top: TSR cross-section. Bottom: representation of variable filling degrees and intermeshing degrees in the cylindrical-polar grid.

The effects of the second screw are implemented in two steps: First, the single screw processing domain is reduced by blocking cells in the intermeshing area. These blockings account for decreasing total reactor volume: The higher the intermeshing degree (decreasing clearance between the shafts), the more cells need to be impenetrable to flow. Reduction of the domain space due to intermeshing of the opposite flights are neglected. Secondly, the counter-rotating type twin screw allows for assumption of a symmetrical velocity distribution between the rotating shafts. Therefore, shear-stress is set to zero in symmetry plane A-A. The bottom of **Figure 1** illustrates typical cross-sections of the actually modelled domains.

The full TSR grid is sketched in **Figure 3**. Reactor dimensions are arbitrarily chosen to meet the demand of a few t/h of mass throughput. For illustration, filling degree is 90 % and intermeshing degree is 40 %. The angular clearance between inlet planes and outlet planes are only for reasons of better visualisation.

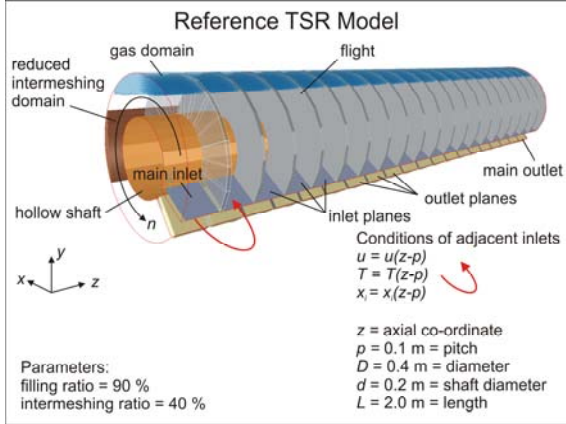


**Figure 3.** TSR reference model in the cylindrical-polar grid.

## Governing Equations

The mathematical model is based upon coupled balance equations of mass, partial mass, momentum and thermal energy. For calculation, an incompressible, steady-state flow of the quasi-homogeneous coal charge is assumed. Gradients inside the coal particles, interactions between solid phase and gas phase, reaction enthalpies of coals, and gravitational forces are not considered.

$$\begin{aligned}
 0 &= -\nabla \cdot \underline{w} \\
 0 &= -\nabla \cdot (\underline{w}\rho_i) + \sum r_{\rho_i} \quad \sum \rho_i = \rho_b \\
 0 &= -\nabla \cdot (\underline{w}\rho_b) - \nabla \cdot \underline{\tau} - \nabla P \\
 0 &= -\nabla \cdot (-\lambda_{eff} \nabla T) - \nabla \cdot (\underline{w}\rho_b c_b T)
 \end{aligned}$$

For formulation of the viscous stress tensor, the non-baking, granular coals are assumed to stay non-cohesive during pyrolysis and as proposed by A.A. Boateng [4], an Ostwald-de-Waele fluid type with quadratic dependency on shear rate is applied. The typically existent yield stress in granular materials is currently not implemented and will be added on later.

## Coal Pyrolysis Kinetics

Coal pyrolysis kinetics is introduced as mass sources and sinks and basically follows the work of D. Merrick [5]. The coals are decomposed in a single, irreversible set of parallel-reactions of first order, while composing char and volatile matter (VM). In dependence on total volatile matter content, up to five parallel reactions are involved. It is important to mention that the individual reactions do not correspond to specific chemical species. Rather, total conversion is described by summing up all reaction rates. While for all coal fractions, the pre-exponential factor is kept

constant, specific and fixed activation energy is selected for each fraction.

$$k_0 = 1.3 \cdot 10^{13} \text{ s}^{-1}$$

$$E_{A,i} = (214; 217; 223; 233; 245) \text{ kJ/mol}$$

The reaction rates for coal, char, and volatile matter are written

$$\begin{aligned}
 r_{\text{coal},i} &= -k_0 \cdot \exp\left(-\frac{E_{A,i}}{RT}\right) \cdot \frac{m_{\text{coal},i}}{V_b} \\
 r_{\text{char},i} &= k_0 \cdot \exp\left(-\frac{E_{A,i}}{RT}\right) \cdot \left(1 - \frac{m_{0,\text{VM},i}}{m_{0,\text{coal},i}}\right) \cdot \frac{m_{\text{coal},i}}{V_b} \\
 r_{\text{VM},i} &= k_0 \cdot \exp\left(-\frac{E_{A,i}}{RT}\right) \cdot \left(\frac{m_{0,\text{VM},i}}{m_{0,\text{coal},i}}\right) \cdot \frac{m_{\text{coal},i}}{V_b}
 \end{aligned}$$

## Thermo-Physical Properties

Specific heat capacity of the solid phase is given by a two-parametric Einstein-equation with characteristic Einstein temperatures of 380 K and 1800 K as determined by D. Merrick [5]. The effective thermal conductivity of the granular coals is expressed applying A. Missenard's [6] model of serial and parallel connections between disperse solid-phase and continuous gas-phase, the latter also including transport due to thermal radiation. Thermal radiation is implemented by means of G. Damköhler's expression for a radiation thermal conductivity. By performing thermal balance and momentum balance between two adjacent layers, comparison of coefficients with Fourier's law of thermal conductivity and Newton's theory of viscosity delivers identical expressions for thermal diffusivity and kinematic viscosity, compare P. Atkins [7].

$$a = \nu = \frac{1}{3} \frac{\lambda}{\rho_b c_b}$$

To obtain maximum momentum transport, it is assumed that a spherical particle meets with a gap in the adjacent layer. The longitudinal distance is assumed to be of particle diameter. If choosing free mean path equal to particle diameter (equal to distance of the two layers), momentum balance leads to the expression

$$\nu_{\text{max}} = d_p^2 \frac{\partial w}{\partial y} = d_p^2 \dot{\gamma} \Rightarrow a_{\text{max}} = d_p^2 \dot{\gamma}$$

Translation of thermal diffusivity into thermal conductivity finally results in

$$\lambda_{\dot{\gamma},\text{max}} = d_p^2 \cdot \dot{\gamma} \cdot \rho_b c_b$$

with quadratic dependency on particle diameter and linear dependency on shear-rate. Predicted effective thermal conductivities are given in **Figure 3**. While the lowest branch, which is effected only by heat-

conduction and thermal-radiation, is in good accordance to experimental results, effective thermal conductivity including the shearing effect seems to be of higher magnitude. For this reason, an experimental set-up to determine the actual impact of shearing is under development.

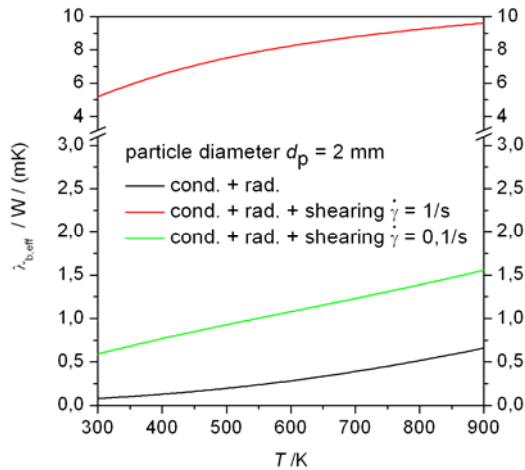


**Figure 2.** Predicted effective thermal conductivities of the quasi-homogeneous granular coal phase

### Boundary Conditions

A first calculation series has been carried out for the fully filled, non-intermeshed reference TSR (**Figure 3**). The coals are assumed to have a volatile matter content of 15 % and a bulk density of 780 kg/m<sup>3</sup>. Further, non-slip boundary conditions and constant wall temperatures of 900 K are applied. Estimation of heat transfer coefficient according to E. Tsotsas and E.-U. Schlünder [8] delivers values of 75 W/m<sup>2</sup>K. The coal enters the reactor at ambient temperature of 300 K. Inlet and outlet pressures are set equal to 10<sup>5</sup> Pa. Gross calorific value of volatile matter is estimated 20 MJ/kg. Starting with this reference model, a comprehensive study of parameters is planned for the future.

### Numerical Computation

The TSR grid is generated by means of a Fortran77 code after the input of the geometric dimensions as the diameters, pitch and the number of rings which finally make up the total length of the screw in co-axial direction. The geometry data are complemented by filling degree, which blocks cells at top of the domain, and intermeshing degree, which blocks cells sideways. Coal fractions are automatically made up in dependence on total volatile matter content of the coals. Afterwards, the set of balance equations is solved steady-state using Phoenics™. To account for numerical stability, a fully implicit upwind scheme is used (H. I. Rosten and D. B. Spalding [9]). Solutions are calculated for radial-, angular- and axial-velocities, temperature, pressure, and partial mass.

## Modelling Results

**Figure 4** summarises total thermal energy balance of the reference TSR. The left ordinate axis designates dimensionless heat flow of flue gas and carried heat flow. The values are normalised, utilising the highest heat flow obtained during the process which is a result of maximum gas evolution at about 4 rpm, resulting in about 160 kW. The right ordinate axis designates dimensionless temperature in which maximum temperature equals wall temperature of 900 K. The lowest branch reflects applied heat flow which increases with rotational speed up to a level at which the heat transfer coefficient becomes limiting. Increased rotational speed is accompanied by continuous decrease of the outlet temperature and due to the chosen boundary conditions, a proportional gain of mass flow. Therefore, the contrary effects of increasing mass throughput while decreasing residence time yield in a local maximum of gas-evolution and therewith, a local maximum of combustion heat flow. Following these results, auto-thermal operation is possible at rotational speeds up to 6 rpm, since thermal energy of the flue gas covers requirement. In this operating range, the TSR process is not limited by insufficient pyrolysis gases. **Figure 4** also illustrates maximum, mean and minimum temperatures at the TSR outlet, characterised by increasing temperature gradient between maximum and minimum temperature with increasing rotational speed. By this prediction, the coals nearby the walls are almost at maximum-temperature, while the coals in the core of the flowing bulk are roughly still at input temperature. By these results, heat transport into the granular coals is the limiting rate.

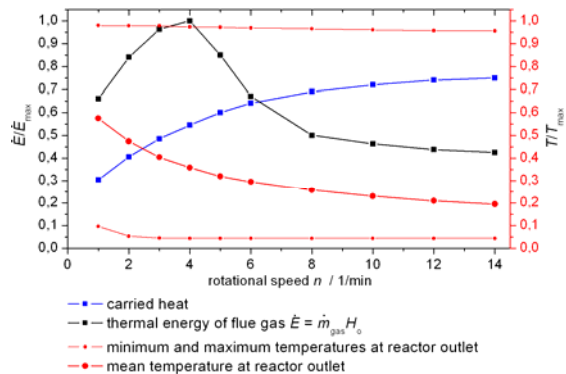


**Figure 4.** Carried heat flow and thermal energy of the flue gas in dependence on rotational speed.

Prediction of mass throughput as a function of filling degree and intermeshing degree is depicted in **Figure 5**. Linear branches indicate theoretical maxima as a consequence of plug flow. Below filling degrees of about 70 %, coal particles don't pass top of the shaft and transport always occurs in c-shaped, closed chambers, although velocity gradients may exist inside the coal charge. If raising filling degree above 70 %, a decrease in mass throughput is observed. This result is an effect of changing transport phenomena, since particles now tend to rotate with the screw due to drag flow. Therewith, total relative



movement between screw and charge is reduced, yielding in a lower throughput (compare with chapter "Single Screw Modelling"). By means of increasing intermeshing degree, the flow pattern is further changed from plug flow into drag flow, thus lowering once more total throughput. Although no functional dependence is implemented yet, it is expected that a sheared charge has a higher potential for effective thermal conductivity due to particle fluctuations at the microscopic scale. In the long run, an appropriate ratio between plug flow and drag flow is to be found, to detect best reactor performance.

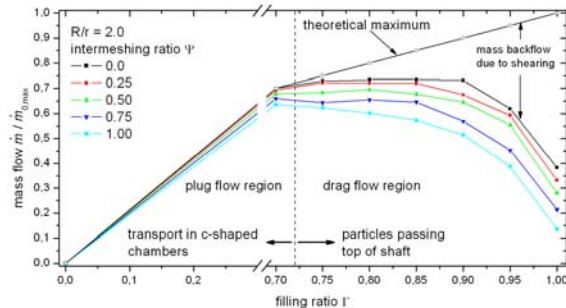


**Figure 5.** Mass flow in dependence on filling degree and intermeshing degree. At filling degrees of roughly higher than 70 %, shafts are covered by the coal charge.

### Experimental Investigations on Heat Transport in Granular Media

The goal of this investigation is to determine the influence of shear-rate on effective thermal conductivity of the coal charge. **Figure 6** demonstrates the set-up of the testing device.

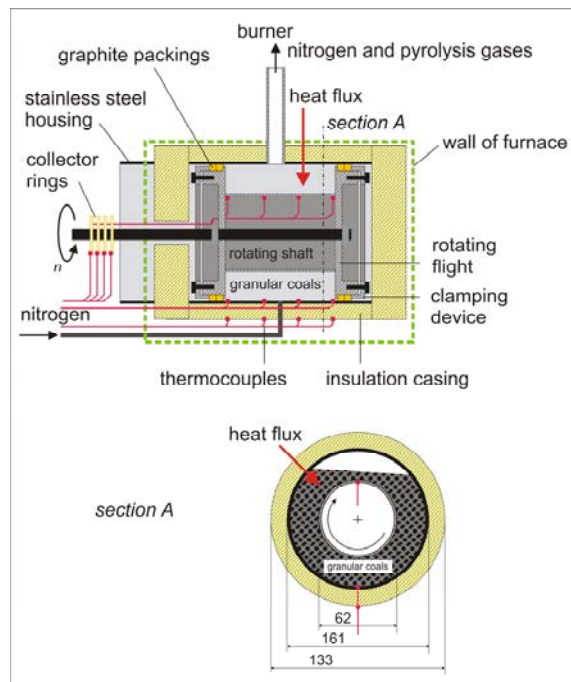


**Figure 6.** Sketch of the testing device for identification of shearing influence on heat transport in granular media.

Granular coals will be indirectly heated-up in a rotating device by a surrounding furnace while measuring wall temperatures of the insulation mantle and the

rotating shaft. With a thermal conductivity of insulation material in the magnitude of 0.1 - 0.5 W/ (mK), heat flux into the coals can be indirectly measured by determination of temperature gradients. Therefore, measuring of temperatures needs to be carried out during the transient phase, i.e. with considerable temperature gradients. Although dominant temperature gradients are expected to appear in the radial direction, a set of four thermocouples will be attached to the insulation mantle and the rotating shaft to account for co-axial heat flux. Since heat flux will be deduced from temperature gradients, all thermocouples have been calibrated in a separate set-up to ascertain validity of the signals. Additional calibration is to be carried out for the collector ring. The insulation is based on calcium silicate. Cutting of the plate-shaped material into annuli was carried out manually with great attention to small tolerances of less than 1 mm with respect to the radial extension. Currently, the set-up is in its final build-up stage. Prior operation, a PAAG/HAZOP security check according to K. Bartels et al. [10] will be necessary. Afterwards, experiments with granular materials of known thermo-physical properties are required for characterisation of process behaviour.

### Conclusion and Future Prospects

By results of calculation carried out for the reference TSR, predicted pyrolysis gases allow for auto-thermal operation at rotational speeds < 6 rpm, unless a coal with very low volatile matter content (<10 %) is chosen. Due to low effective thermal conductivities in the range of 0.1 - 0.5 W/ (mK) and poor radial particle movement, coal particles nearby hot walls are almost fully pyrolysed, while the core of the charge is still cold. As a first result, the TSR process is limited by heat transport through the granular charge.

Currently, two mixing effects are not implemented in the model due to lacking information: Dispersive mixing due to shearing, which occurs inside the charge and free particle movement at the charge surface under influence of gravitational forces, which contributes both to dispersive and distributive mixing. A theoretical maximum for effective thermal conductivities of the sheared charge delivers values five times higher at shear-rate of 1/s and 2 mm particle diameter, than without shearing. To validate this result, the actual impact of shearing will be tested in an experimental set-up. The next steps in TSR modelling will be to complement the generalised Newtonian fluid by a yield stress to account for more realistic flow behaviour of the non-cohesive, granular coals. Non-slip boundary conditions will be replaced by slip boundary conditions and instead of constant wall temperatures, a counter-flow heat transfer calculation will be implemented to verify auto-thermal operation.

### Acknowledgement

The present work is part of the ULCOS program, which operates with direct financing from its 48 partners, especially of its core members (Arcelor-Mittal, Corus, TKS, Riva, Voestalpine, LKAB, Saar-

stahl, Dillinger Hütte, SSAB, Ruukki and Statoi), and has received grants from the European Commission under the 6<sup>th</sup> Framework RTD program and the RFCS program<sup>1</sup>.

## Nomenclature

Symbol	Units	Description
$a$	$\text{m}^2/\text{s}$	thermal diffusivity
$c_b$	$\text{J}/(\text{kg K})$	specific heat capacity of coal bulk
$c_s$	$\text{J}/(\text{kg K})$	specific heat capacity of solid coal particle
$d_p$	$\text{m}$	particle diameter
$E_{A,i}$	$\text{J}/\text{mol}$	activation energy of fraction $i$
$H_o$	$\text{J}/\text{kg}$	gross calorific value
$k_0$	$1/\text{s}$	pre-exponential factor
$m_{0,i}$	$\text{kg}$	initial partial mass $i$
$P$	$\text{Pa}$	pressure
$r_{\rho_i}$	$\text{kg}/(\text{m}^3 \text{ s})$	reaction rate of fraction $i$
$R$	$\text{J}/(\text{mol K})$	gas constant
$T$	$\text{K}$	temperature
$V_b$	$\text{m}^3$	volume of balance
$\underline{w}$	$\text{m}/\text{s}$	velocity vector
$\bar{w}$	$\text{m}/\text{s}$	mean speed
$\varepsilon$	1	interparticle porosity
$\dot{\gamma}$	$1/\text{s}$	shear-rate
$\lambda_{\text{eff}}$	$\text{W}/(\text{mK})$	effective thermal conductivity
$\Lambda$	$\text{m}$	free mean path
$\nu$	$\text{m}^2/\text{s}$	kinematic viscosity
$\underline{\tau}$	$\text{Pa}$	viscous stress tensor
$\rho_b$	$\text{kg}/\text{m}^3$	bulk density (coal charge density)
$\rho_i$	$\text{kg}/\text{m}^3$	density of partial mass $i$
$\rho_s$	$\text{kg}/\text{m}^3$	density of solid coal particle
$\psi$	1	intermeshing degree
$\Gamma$	1	filling degree

## References

- [1] Denys, M. B.; Smith, B.: October 2006, *Proposal SP11 New Advanced Carbon-Based Steel Production*. Corus Research, Development & Technology
- [2] Marth, J.: *Zur Bestimmung der effektiven Wärmeleitfähigkeit von Kohlenschüttungen und ihren Pyrolyseprodukten bei Temperaturen von 150 ° bis 550 ° C*, Ph.D., Berlin University of Technology

[3] Hensen, F.; Knappe W.; Potente H.: 1989, *Handbuch der Kunststoff-Extrusionstechnik*, Carl Hanser Verlag München, Wien. ISBN 3-446-14340-8

[4] Boateng, A.A.: 1993, *Rotary Kiln Transport Phenomena — Study of the Bed Motion and Heat Transfer*, PhD Thesis. The University of British Columbia

[5] Merrick, D.: 1977, *Metallurgical Coke Manufacture: A Mathematical Study*, PhD Thesis, University of London

[6] Missenard, A.: 1965, *Conductivité thermique des solides, liquides, gaz et de leurs melanges*, Paris

[7] Atkins, P.: 2002, *Atkins' Physical Chemistry*, Oxford University Press

[8] Tsotsas, E. ; Schlünder, E.-U. : 1991, *VDI-Wärmeatlas, Wärmeübergang von einer Heizfläche an ruhende oder mechanisch durchmischte Schüttungen*, VDI-Verlag, Düsseldorf

[9] Rosten, H. I., Spalding, D. B.: 1987, *The Phoenix Beginner's Guide*, CHAM, Wimbledon, England

[10] Bartels, K.; Hoffmann H.; Rossinelli, L., 1990: *PAAG-Verfahren (HAZOP)*, Internationale Sektion der IVSS für die Verhütung von Arbeitsunfällen und Berufskrankheiten in der chemischen Industrie

<sup>1</sup> Priority 3 of the 6<sup>th</sup> Framework Programme in the area of "Very low CO<sub>2</sub> Steel Processes", in co-ordination with the 2003 and 2004 calls of the Research Fund for Coal and Steel